The Journal of Infectious Diseases

MAJOR ARTICLE

Preclinical Pharmacological Development of Chlorcyclizine Derivatives for the Treatment of Hepatitis C Virus Infection

Adam Rolt,[1] Derek Le,[1] Zongyi Hu,[1] Amy Q. Wang,[2] Pranav Shah,[2] Marc Singleton,[2] Emma Hughes,[2] Andrés E. Dulcey,[2] Shanshan He,[1] Michio Imamura,[3] Takuro Uchida,[3] Kazuaki Chayama,[3] Xin Xu,[2] Juan J. Marugan,[2] and T. Jake Liang[1]

[1]Liver Diseases Branch, National Institute of Diabetes and Digestive and Kidney Diseases, National Institutes of Health, Bethesda, Maryland; [2]Division of Pre-Clinical Innovations, National Center for Advancing Translational Sciences, National Institutes of Health, Rockville, Maryland; and [3]Department of Medicine and Molecular Sciences, Graduate School of Biomedical Sciences, Hiroshima University, Japan

Hepatitis C virus (HCV) is a small, single-stranded, positive-sense RNA virus that infects more than an estimated 70 million people worldwide. Untreated, persistent HCV infection often results in chronic hepatitis, cirrhosis, or liver failure, with progression to hepatocellular carcinoma. Current anti-HCV regimens comprising direct acting antivirals (DAAs) can provide curative treatment; however, due to high costs there remains a need for effective, shorter-duration, and affordable treatments. Recently, we disclosed anti-HCV activity of the cheap antihistamine chlorcyclizine, targeting viral entry. Following our hit-to-lead optimization campaign, we report evaluation of preclinical in vitro absorption, distribution, metabolism, and excretion properties, and in vivo pharmacokinetic profiles of lead compounds. This led to selection of a new lead compound and evaluation of efficacy in chimeric mice engrafted with primary human hepatocytes infected with HCV. Further development and incorporation of this compound into DAA regimens has the potential to improve treatment efficacy, affordability, and accessibility.

Keywords. antiviral; lead compound; drug development; pharmacokinetics.

Hepatitis C virus (HCV) is a small, single-stranded, positive-sense RNA virus that infects more than an estimated 70 million people worldwide [1]. HCV is transmitted by direct blood-to-blood or other percutaneous contact, with a significant proportion of the infected population unaware of their infection status due to the often-asymptomatic onset. Persistent infection with HCV results in chronic hepatitis and liver diseases such as hepatocellular carcinoma, cirrhosis, or liver failure; liver transplantation following acute liver failure is accompanied by universal allograft reinfection. Greater than 50% of hepatocellular carcinoma diagnoses and approximately 54000 deaths per year are associated with chronic HCV infection [1].

With the aim of improving on the cornerstone of treatment that comprised interferon-α and ribavirin, 2011 saw the introduction of the first-generation direct-acting antivirals (DAAs) targeted specifically towards nonstructural viral proteins NS3/4A, NS5B, and NS5A [2–5]. Contemporary interferon-sparing all-oral regimens, consisting of DAA combinations such as Harvoni, Viekira Pak, Technivie, and others, produce sustained virologic response (SVR) rates above 90% in clinical studies; however, effectiveness in real-world scenarios has proven to be less consistent [6–11].

While the SVR rate per treatment course has improved dramatically, the cost per SVR has in fact unfortunately increased in parallel [4, 12, 13]. The increase in cost, coupled with pressure on health care providers to make these new therapies available, results in an increasing burden on health care systems in developed countries, and under-utilization in developing countries. Therefore, the development of new therapeutic agents towards HCV to use in combination therapies will not only serve to increase pangenotypic efficacy and further decrease the chances for resistance development, but it will also ensure affordability, allowing populations that are most affected by HCV to benefit from the treatments. Following our discovery that the approved antihistamine chlorcyclizine is a potent inhibitor of HCV in animal models, a chemical optimization campaign towards improved chlorcyclizine derivatives was undertaken [14, 15]. We present here an analysis of the in vitro efficacy, absorption, distribution, metabolism, and excretion (ADME) properties, and in vivo pharmacokinetic properties of several lead molecules, evaluation of anti-HCV efficacy of a lead compound in an animal model of HCV infection, and a discussion of preclinical selection with future direction.

METHODS

HCV-Luc Infection Assay and ATPlite Assay

Huh7.5.1 cells were seeded in 96-well plates (10^4 cells/well) and cultured overnight. HCV-Luc was used to infect Huh7.5.1 cells

Received 7 September 2017; editorial decision 10 January 2018; accepted 17 January 2018; published online January 24, 2018.

Correspondence: T. J. Liang, MD, Liver Diseases Branch, National Institute of Diabetes and Digestive and Kidney Diseases, National Institutes of Health, Bethesda, Maryland (jliang@nih.gov).

The Journal of Infectious Diseases® 2018;217:1761–9

DOI: 10.1093/infdis/jiy039

in the presence of increasing concentration of tested compound. Viral infection and replication were measured by luciferase signal 48 hours after treatment using the *Renilla* luciferase assay system (Promega). Cytotoxicity in Huh7.5.1, HepG2, primary human hepatocytes, and MT-4 cells was evaluated by the ATP-based cell viability assay with ATPlite assay kit (PerkinElmer). The concentration values that lead to 50% and 90% viral inhibition (EC_{50} and EC_{90}) and 50% cytotoxicity (CC_{50}) were calculated with GraphPad Prism 5.0 software (GraphPad Software Inc.) using nonlinear regression analysis. Production of chimeric HCV genotype viruses (C-E1-E2-p7-NS2 sequences of genotypes 1a, 1b, 2a, 2b, 3a, 4a, 5a, 6a, and 7a in the backbone of JFH1 strain) containing a *Renilla* luciferase reporter have been described previously [16].

β-Arrestin H1-Histamine Receptor Assay

H1-histamine receptor assay was carried out with the PathHunter β-Arrestin GPCR Assay kit following the antagonist procedure (DiscoveRx). The PathHunter cells were plated in 384-well plates and cultured overnight before adding the compound of interest. After incubation for 30 minutes, agonist histamine (0.25 μM) was added and plates were incubated for additional 120 minutes before adding detection solution. Chemiluminescence was read after 60 minutes incubation at room temperature. Percent antihistamine activity was calculated based on the result from histamine-treated wells.

High-Throughput Microsomal Stability Assay

Multiple time-point metabolic stability assay was run in triplicates using the substrate depletion method or the in vitro half-life ($t_{1/2}$) method. Sample analysis and half-life determinations were performed using previously described method [17].

High-Throughput Kinetic Solubility Assay

Pion's patented μSOL assay for kinetic solubility determination was used. In this assay, the classical saturation shake-flask solubility method was adapted to a 96-well microtiter plate format and a cosolvent method with n-propanol as the reference compound was utilized. Test compounds were prepared in 10 mM dimethyl sulfoxide (DMSO) solutions (45 μL), and diluted with the cosolvent to a final drug concentration of 150 μM in the aqueous solution (pH 7.4). Samples were incubated at room temperature for 6 hours to achieve equilibrium. The samples were then filtered to remove any precipitate formed. The concentration of the compound in the filtrate was measured by UV absorbance. The reference drug concentration of 17 μM was used for quantitation of unknown.

High-Throughput PAMPA Permeability Assay

The effective permeability of compounds was determined via passive diffusion using the stirring double-sink parallel artificial membrane permeability assay (PAMPA) method from pION Inc. (www.pion-inc.com), with a fully automated system of sample preparation, sample analysis, and data processing, as described previously [18].

In Vivo Pharmacokinetics

Male CD-1 mice (approximately 35 g) were obtained from Charles River Laboratories (Wilmington, MA). Mice were housed at the centralized animal facilities at the National Institutes of Health (NIH, Bethesda, MD) with a 12-hours light-dark cycle. The housing temperature and relative humidity were monitored based on the Standard Operating Procedure issued by NIH Division of Veterinary Resources (DVR). The animals had free access to water and food. All experimental procedures were approved by the Animal Care and Use Committee of the NIH DVR. The dosing solution of a test compound was freshly prepared prior to the drug administration in 50% propylene glycol and 50% water. The pharmacokinetics was evaluated after single administration at the stated dosage and route (ie, oral gavage [PO], intravenous [IV], or intraperitoneal [IP] injection). The blood and liver samples were collected at predose, 0.083, 0.25, 0.5, 1, 2, 4, 7, and 24 hours. Three animals (n = 3) were sacrificed at each time point and blood and liver samples were collected. Plasma samples were harvested after centrifugation of blood samples at room temperature. Plasma and liver samples were frozen immediately after collection, and stored at −80°C prior to sample analysis. The concentrations of a test compound in the plasma and liver were determined by ultraperformance liquid chromatography-mass spectrometry analysis (UPLC-MS/MS). The mean concentrations from 3 animals at each time point were used in the PK calculation. The pharmacokinetic parameters were calculated using the noncompartmental method (Model 200 for oral or IP administration and Model 201 for IV administration) of the pharmacokinetic software package Phoenix WinNonlin, version 6.2 (Certara, St. Louis, MO). The area under the plasma and liver concentration versus time curve (AUC) was calculated using the linear trapezoidal method. Where warranted, the slope of the apparent terminal phase was estimated by log linear regression using at least 3 data points, and the terminal rate constant (λ) was derived from the slope. $AUC_{0-\infty}$ was estimated as the sum of the AUC_{0-t} (where t is the time of the last measurable concentration) and $C_{t/\lambda}$. The apparent terminal half-life ($t_{1/2}$) was calculated as 0.693/λ. The oral bioavailability was estimated from the dose normalized AUC ratio between IV and oral administration. The maximum concentration (C_{max}) and time to reach C_{max} (T_{max}) were also reported.

In Vivo Efficacy Studies in Chimeric Mouse Model

Alb-uPA/SCID mice were engrafted with primary human hepatocytes and then infected with HCV serum samples of genotype 1b (10^5 HCV copies) as described previously [14]. The mice were monitored for serum HCV RNA and human albumin for 6 weeks before treatment. Genotype 1b HCV titers

were monitored in HCV-infected chimeric mice over a 4-week period of treatment with various compounds; human serum albumin was measured in parallel for control.

RESULTS

In Vitro Anti-HCV Activities and ADME Properties

Table 1 describes the structure, in vitro anti-HCV activity, and ADME properties of current lead compounds in the chlorcyclizine (CCZ) series [15]. In order to determine which analogues to advance to in vivo pharmacokinetic analysis, candidates were distinguished based on their in vitro ADME properties in combination with anti-HCV activity. The anti-HCV activity of the compounds was assessed using the cell-based HCV-Luc infection assay, utilizing HCV-JFH1 harboring a luciferase reporter in the p7 region, and is expressed as the EC_{50} (the concentration of compound required to reduce HCV viral load by 50% compared to a negative control). Cytotoxicity was evaluated using an ATPlite assay and is designated as CC_{50} (the concentration of compound exhibiting 50% cytotoxicity compared to a negative control). Both assays were carried out in the Huh7.5.1 cell line and utilized DMSO as a negative control. The relationship between EC_{50} and CC_{50} is described by a selectivity index (SI) representing the fold-difference between the 2 values. Cytotoxicity was further evaluated in other cell culture systems including primary human hepatocytes, HepG2, and MT-4 (human T-cell leukemia) cell lines. These compounds showed comparable CC_{50} in these cells (Table 1).

The lead compounds described in Table 1 are potent inhibitors of HCV with concomitant low toxicity; most notably compound 3 displays the highest potency, resulting in a large selectivity index (EC_{50} = 2.3 nM, CC_{50} = 19.8 μM, SI = 8609). In contrast to the original hit compound CCZ (entry 1), the lead compounds are achiral (R^1 = R^2 = Cl), which simplifies synthesis and interpretation of biological results. Alkyl analogues at the piperazine nitrogen, entries 2–6, possess similarly long metabolic half-lives ($t_{1/2}$) in human microsomes, comparable kinetic solubility, and permeability compared to CCZ, but with increased potency and improved selectivity (SI). Pegylated analogues 7–12 maintain potency and selectivity, and display an overall increase in solubility while preserving cell permeability.

CCZ is primarily indicated for use as an antihistamine, the effect of which is mediated through H1 histamine receptor (H1HR) antagonism, and so our lead compounds should ideally display weaker histamine receptor antagonism to reduce the likelihood of off-target effects for anti-HCV development. The H_1 histamine receptor antagonistic activities of the lead compounds in Table 1 were evaluated by measuring their capacity to block the β-arrestin internalization signal induced by histamine. Values are reported as a residual percentage of maximal activation induced by the agonist histamine at 250 nM in the presence of 10 nM of the selected CCZ derivatives (normalized to DMSO as a negative control, 100% activation). Accordingly, all compounds in Table 1 displayed reduced histamine receptor antagonism (higher % of H1HR activities) compared to (R)-CCZ or racemic-CCZ (16% of H1HR activity).

In our previous study, CCZ exhibited varying activities against different HCV genotypes, with most-potent activity against genotypes 2 [14]. We thus tested compound 3, the most active compound here, against various chimeric HCV genotype viruses. As shown in Table 2 and Supplementary Figure 1, compound 3 is most active against genotype 2 (EC_{50} in nM range) but much less active against other genotypes (EC_{50} in μM range). Thus there was no improvement in a broader genotypic coverage.

Pharmacokinetic Profiles

Based on our interpretation of the in vitro ADME profiles, 6 candidates were chosen for further investigation. Pharmacokinetic studies were performed on these derivatives (Figure 1 and Table 2), elucidating the in vivo properties of these compounds in order to select derivatives to be used in mouse efficacy studies, and to develop a dosing regimen. For single IP injection, the compounds were derivatized as di-trifluoroacetate (TFA) salts, which could be solubilized in a solution of 1:1 propylene glycol and water for administrations at 1 mg/mL. Following single IP administration, plasma and liver levels of the compounds were determined at set time-points over the course of 24 hours. Summaries of the salient properties of the selected leads in these experiments are described in Table 3.

Studying the elimination profiles of the 6 compounds investigated allows their separation into 2 distinct categories (Figure 1). Compounds 1, 2, 3, and 7 exhibited classical 2-phase distribution and elimination kinetics; the maximum concentrations of these compounds in plasma and in the liver occurred within 15 minutes of administration, which was followed by a slower elimination phase.

Compounds 9 and 12 did not display any significant elimination phase in liver and appeared to become increasingly localized and subsequently trapped in the liver over the course of the experiment. The liver-specific accumulation of compounds 9 and 12 was not observed to reverse over a study period of 7 days or by reducing the dose to 0.1 mg/kg, thus making them unsuitable for further investigation. The extended retention of these 2 compounds in the liver becomes problematic when considering appropriate dosing selection and potential long-term toxicity. Compound 12 also exhibited higher cytotoxicity in cell cultures (Table 1). Similar to CCZ, compounds 2, 3, and 7 maintained comparable levels of exposure (AUC) and favorable liver localization, but with improved in vivo half-lives in all cases. Ethyl substituted derivative compound 3 exhibited marked improvement in comparison between liver C_{max}/EC_{50}. This feature, coupled with an in vivo half-life that would be suitable for daily dosing and a liver to plasma ratio of approximately 20:1, led us to select compound 3 as our lead for investigation in efficacy studies in vivo.

Table 1. The Structure, In Vitro Anti-Hepatitis C Virus (HCV) Activity, and ADME Properties of Current Lead Compounds in the Chlorcyclizine (CCZ) Series

Chemical structure

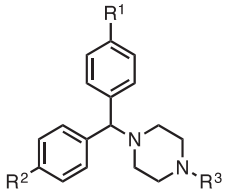

				Anti-HCV activity and selectivity						ADME properties				
					[c]CC_{50} (μM)						Microsomal $t_{1/2}$ (min)			
Cmpd.	R^1	R^2	[a]R^3	[b]EC_{50} (nM)	Huh-7.5.1	Hep G2	MT4	PHH	Selectivity Index[d]	H_1HR %DMSO at 10 nM[e]	Human	Mouse	Rat	Permeability (10^{-6} cm/s)	Solubility (μg/mL)
1	Cl	H		24	33.4	32.34	19.55	32.9	1392	79.4	>30	26.1	2.1	1834.0	29.3
2	Cl	Cl		17 ± 6.1	21.3	ND	ND	27	1253	52.2	>30	>30	26.0	1024.3	49.0
3	Cl	Cl		2.3 ± 0.9	19.8	56.03	24.8	24.3	8609	71.8	>30	12.6	2.2	892.3	17.7
4	Cl	Cl		8.0 ± 1.9	29.3	ND	ND	ND	4651	96.9	>30	6.6	1.9	ND	7.3
5	Cl	Cl		8.6 ± 2.5	25.1	ND	ND	ND	6436	102.4	>30	19.7	1.7	2215.6	9.2
6	Cl	Cl		34.2 ± 16.2	26.2	ND	ND	ND	7486	100.8	>30	7.0	1.8	ND	4.0
7	Cl	Cl		9.9 ± 5.6	19.7	19.53	14.65	ND	1990	52.6	>30	10.0	13.7	856.0	44.5
8	Cl	Cl		51.5 ± 17.2	ND	55.58	25.03	13.2	ND	33.2	11.2	5.4	8.1	616.3	15.8
9	Cl	Cl		31.0 ± 5.3	29.7	ND	2.55	3.76	958	47.9	ND	ND	>30.0	2266.0	43.1
10	Cl	Cl		85.0 ± 6.2	24.2	23.23	17.09	17	285	45.9	5.2	2.5	4.8	1900.0	59.7
11	Cl			148 ± 27.6	ND	21.33	25.57	21.6	ND	88.7	ND	ND	5.3	421.2	65.2
12	Cl	Cl		23 ± 4.9	8.13	23.23	3.75	3.95	3535	72.3	>30	>30	>30.0	ND	80.0

[a] Me, methyl; Et, ethyl; ^{n}Pr, ^{n}propyl; ^{i}Pr, isopropyl.

[b] 50% viral inhibition (EC_{50}) ± standard error of the mean (SEM) ($n \geq 3$) from the HCV-Luc infection assay.

[c] 50% cytotoxicity (CC_{50}) from the ATPlite cytotoxicity assay.

[d] Selectivity index = CC_{50} (Huh-7.5.1) /EC_{50}.

[e] Residual H_1 histamine receptor activity (H_1HR) expressed as % of dimethyl sulfoxide (DMSO) negative control at 10 nM concentration. H_1HR activity of racemic CCZ at 10 nM, of 16% DMSO control.

Abbreviations: ADME, absorption, distribution, metabolism, and excretion; Cmpd, compound; PHH, primary human hepatocytes; ND, not determined.

Table 2. The EC_{50} and CC_{50} of Compound 3 Against each Hepatitis C Virus (HCV) Chimeric Genotype, Determined as Described in the Methods and Shown in Detail in Supplementary Figure 1

	HCV Chimeric Genotype								
	1a	1b	2a	2b	3a	4a	5a	6a	7a
EC_{50} (μM)	12.55	6.24	0.00059	0.0080	8.11	8.99	9.465	6.47	10.99
CC_{50} (μM)	25.11	14.02	26.42	26.54	26.06	26.64	25.85	22.18	26.9

Abbreviations: EC_{50}, 50% viral inhibition; CC_{50}, 50% cytotoxicity.

Pharmacokinetics of Compound 3

In order to establish an appropriate dosage for daily administration of compound 3, further investigation into the relationship between dose and pharmacokinetic profile were conducted. For IP, IV, and PO administration, compound 3 was formulated as a 1:1 oxalate salt, which can be solubilized in a 1:1 solution of propylene glycol and water at a concentration at 1 mg/mL for administration.

Concerning exposure and kinetic profiles, an overall approximate linear relationship is observed between different dosages and extravascular routes of administration (ie, IP or PO) after accounting for oral bioavailability. Comparing PO administrations of compound 3, a 10-fold decrease in dose translated linearly to a 10-fold decrease in exposure in the liver with similar half-lives and elimination profiles (AUC_{∞} /D for 10 mg/kg and 1 mg/kg administration = 5920 h·μM and 6320 h·μM, respectively; $t_{1/2}$ = 3.7 and 3.2 hours, respectively). Compound 3 significantly localized to the liver as opposed to the heart or brain when C_{max} values for these tissues were compared. The overall exposure in the liver was much higher than that in plasma, with a liver to plasma ratio of 23:1 following PO administration. Analysis of the PK data following IV and PO administration revealed an oral bioavailability of 55% at 10 mg/kg and a steady state volume of distribution (V_{dss}) of 11 L/kg. These data indicate that the compound had a good oral bioavailability and a preferential compartmentalization into body tissues, recapitulating the observed liver distribution. Serum alkaline phosphatase (ALK), alanine transaminase (ALT), and aspartate transaminase (AST) levels throughout the 24 hours following IP administration at 10 mg/kg were determined as markers of hepatotoxicity. Figure 2C shows a transient elevation (1 time point) of ALT (similarly for AST, not shown) before decreasing to pretreatment levels over 24 hours in 1 mouse; ALK levels remained within the normal limit of the assay throughout the course of the experiment (<5 U/L). Vehicle control-treated mice also showed occasional increases in ALT values (Figure 2D) [15]. We thus considered this observed increase as probably unrelated to the compound.

In Vivo Anti-HCV Efficacy of Compound 3

The anti-HCV efficacy of compound 3 was analyzed in vivo in an albumin–urokinase plasminogen activator/severe combined immune-deficient (*Alb-uPA/SCID/bg*) chimeric mouse model infected with HCV genotype 1b [14]. HCV viral load was monitored over the course of treatment, along with measurement of human serum albumin as a control. Based on the pharmacokinetic data, a dose of 5 mg/kg administered IP daily was chosen for the "proof of concept" efficacy study. Administration of compound 3 in this manner was associated with a time-dependent reduction

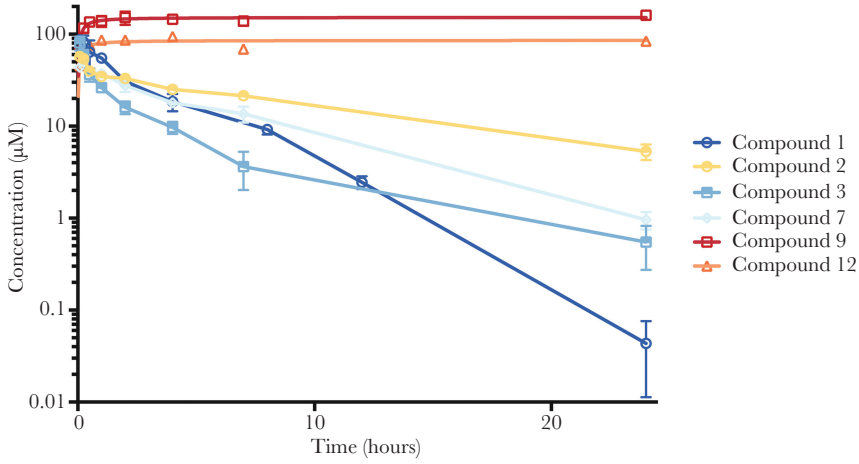

Figure 1. Mouse liver concentration-time profiles of 6 lead CCZ derivatives. Following preparation of the selected compound at a dosing concentration of 1 mg/mL in 50% propylene glycol and 50% water, the pharmacokinetics were evaluated after single intraperitoneal administration at 10 mg/kg. The blood and liver samples were collected at predose, 0.083, 0.25, 0.5, 1, 2, 4, 7, and 24 hours (n = 3). The concentrations of the compound in the plasma and liver were determined by ultraperformance liquid chromatography-mass spectrometry analysis, as described in the Materials and Methods.

Table 3. Properties of the Selected Lead Compounds

	Plasma					Liver						
Cmpd.	T_{Max} (h)	C_{Max} (μM)	$T_{1/2}$ (h)	AUC_{24h} (h·μM)	[b]AUC_{∞} (h·μM)	T_{Max} (h)	C_{Max} (μM)	$T_{1/2}$ (h)	AUC_{24h} (h·μM)	[b]AUC_{∞} (h·μM)	Liver/Plasma Ratio[c]	C_{Max}/EC_{50}[d]
1a	0.25	3.2	2.0	9.8	9.8	0.083	87	2.0	262.3	262.5	26.8	3.6
2	0.083	5.3	6.7	27.6	29.9	0.083	54.7	8.5	431.1	497.0	15.6	3.2
3	0.083	3.5	4.7	7.3	7.5	0.083	80.43	4.8	145.1	149.0	19.9	35.0
7	0.25	6.9	2.6	27.2	27.2	0.25	52.6	4.6	289.1	296.5	10.6	5.3
9	0.083	1.8	12.0	2.9	3.6	24	161.12	ND	3536.8	ND	1231.0	5.4
12	0.083	6.9	15.3	8.0	9.8	4	95.98	ND	1908.4	ND	239.9	3.4

[a] 50 mg/kg dosage. AUC_{24}, AUC_{∞}' and C_{Max} have been reduced to one-fifth of their measured value for comparison.

[b] Extrapolated total exposure from a single dose.

[c] Ratio of AUC_{24}.

[d] 50% viral inhibition (EC_{50}), see Table 1.

Abbreviations: AUC_{∞}, area under the curve extrapolated from time 0 to infinity (total compound exposure); AUC_{24h}, area under the curve (compound exposure) from time 0 to 24h; C_{Max}, maximum concentration; Cmpd, compound; ND, not determined; T_{Max} time to reach C_{max}; $T_{1/2}$, half-life.

of HCV virus load of approximately 1 log_{10} from the initial HCV virus titer after 4 weeks in 3 of 4 mice (Figure 3A, mice 1–3) with no observable toxicity. Mouse 4 (Figure 3A) had an initial 0.6-log decrease in viral level and then rebounded to pretreatment level. In comparison, untreated control mice showed steady viral levels during the same time frame of observation (Figure 3C). A parallel evaluation of the NS3 inhibitor asunaprevir revealed an initial potent antiviral effect followed by a rebound (Figure 3B), likely representing emergence of drug-resistant mutants [19, 20]. Throughout the experiment, all mice showed steady levels of human serum albumin in the blood (Figure 3, lower panels).

The average terminal concentrations of the parent drug in the liver after the 4-week administration period were approximately 1000-fold the IC_{50} (2.32 μM and 2.3 nM, respectively). Additionally, an even greater concentration of the des-ethyl metabolite was observed, itself a potent anti-HCV compound in

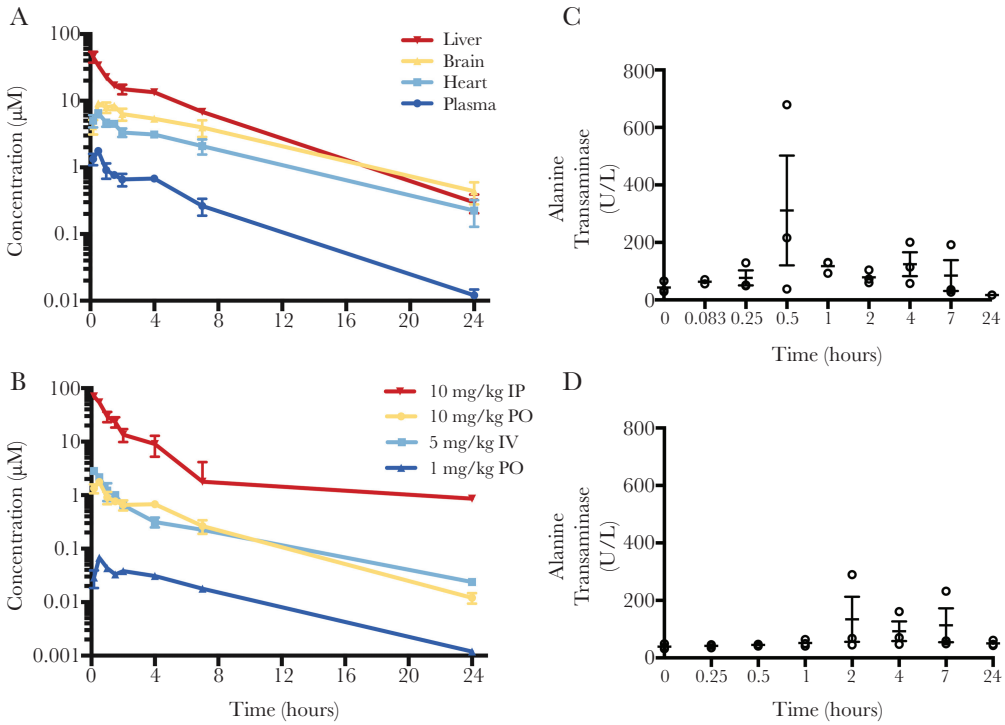

Figure 2. Pharmacokinetic profile of compound 3. *A*, Tissue-specific distribution of compound 3 following 10 mg/kg oral (PO) administration over 24 hours. *B*, Establishing linearity of exposure between 10 mg/kg and 1 mg/kg doses in plasma. Intravenous (IV) administration was used to calculate bioavailability (F) and volume of distribution (V_{dss}). Plasma levels of alanine transaminase (ALT; *C*) were determined at several time points over the treatment window following 10 mg/kg intraperitoneal (IP) administration as an indicator of drug-related hepatotoxicity; T_0 = pretreatment. *D*, Vehicle-only control showing spotty increases in alanine transaminase unrelated to administration of the compound.

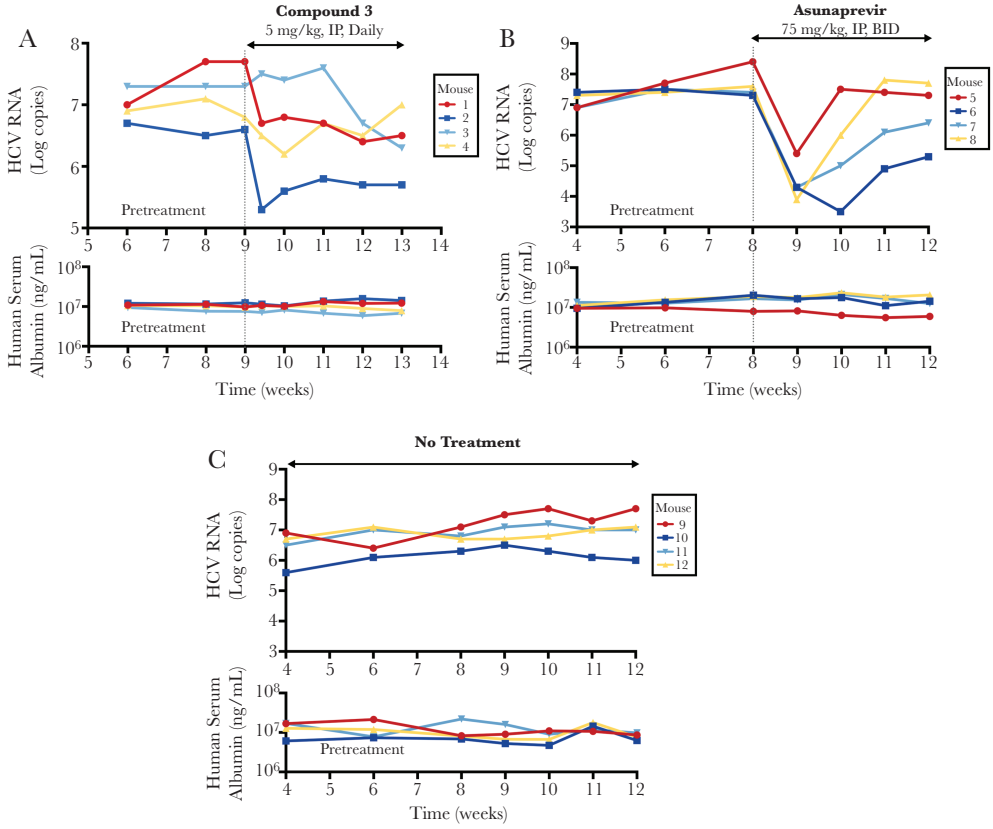

Figure 3. In vivo efficacy of compound 3 (5 mg/kg, intraperitoneal [IP], daily) in comparison to asunaprevir (75 mg/kg, oral, twice a day [BID]) and a no treatment control over a 4-week administration period, and quantification of biomarkers associated with hepatotoxicity. *Alb-uPA/SCID* mice were engrafted with primary human hepatocytes and infected with hepatitis C virus (HCV) of genotype 1b (10^5 HCV copies). The mice were monitored for serum HCV RNA and human albumin for 4 weeks pre- and post-treatment. *A, B, C,* The upper panels represent changes over time in the genotype 1b HCV titers (Log copies) from pretreatment levels with compound 3, asunaprevir, or no treatment, respectively. The lower panels are respective human serum albumin levels over the course of the experiment.

vitro (18.9 μM terminal concentration, EC_{50} 33 nM, 573-fold difference). Terminal liver concentrations were 35-fold greater than the average peak plasma concentration throughout the course of the experiment; this observation is in line with the previously outlined distribution data from single-dose pharmacokinetic experiments. Specifically, mouse 4 (Figure 3A) was exposed to above average concentrations of compound 3 in terminal liver samples (2.72 μM), and so the reason for viral rebound is not clear. It is possible that this rebound may represent emergence of CCZ-resistant mutations. Throughout the course of the experiment, there was no observed weight loss, hair loss, decreased food intake, or reduced activity, indicating no general toxicity.

CONCLUSIONS

The development of contemporary anti-HCV therapies is a success story of modern medicinal chemistry but due to high cost they are underutilized. Therapeutic regimens are not chosen solely based on patient needs but are determined by what resources are available from the point of view of the health care provider. Advancements in HCV cell culture systems allowed us to approach this problem from a phenotypic perspective, to develop treatments that have a different mode of action from the existing DAAs, and are thus likely synergistic with currently available drugs due to their mechanism of action [21–23]. We have previously shown that CCZ inhibits the entry step of HCV infection and exhibits synergistic activity with currently approved anti-HCV agents in vitro [14, 24]. The mechanism of action of CCZ and related compounds has been proposed to target the fusion process of viral entry, possibly involving the fusion loop sequence of the HCV E1 protein [25].

Alterations to the piperazine ring of the CCZ scaffold were found to decrease activity; however, substitutions on the terminal nitrogen (Table 1, R_3) were tolerated while maintaining potency. This was utilized functionally as a handle to develop the in vitro ADME profile of the CCZ analogues before moving selected analogues forwards for in vivo studies, without adversely affecting the EC_{50}.

Pegylated derivatives 9 and 12 were observed to heavily localize to the liver; drawing comparison, particularly between compounds 7–12 suggests that the localization in the liver of compounds 9 and 12 is in fact due to the presence of the primary amine on the PEG chain. Lipophilic cationic amphiphiles such as CCZ possessing basic amine moieties can become trapped in acidic (pH < 5) subcellular compartments such as lysosomes. This can lead to specific accumulation in lysosome-rich organs

such as the liver, which is represented in the large volume of distribution [26, 27]. Generally, liver localization and accumulation may be thought of as undesirable; however, because HCV infects only hepatocytes, we regard the liver as the target organ and hence modest accumulation as favorable.

In mice that positively responded to treatment with compound 3 at a dose of 5 mg/kg daily, approximately a 1-log drop in viral load could be affected, which is similar to what we observed previously with CCZ at 10–50 mg/kg daily dosing. It is possible that a lower dose of compound 3 may be equally efficacious because of its longer half-life and more potent $EC_{50.}$ There was no evidence of toxicity at this dose for 4 weeks.

In summary, the work presented here reinforces the potential utility of CCZ and analogues for treatment of HCV. A thorough evaluation of in vitro ADME of derivatives of CCZ followed by in vivo pharmacokinetic investigations led to the selection of compound 3 as an anti-HCV lead, which resulted in approximately a 1 $\log_{10}$ or 90% drop in HCV virus load at a dose of 5 mg/kg daily over 4 weeks in a time-dependent manner. Coupled with the observation that CCZ has been demonstrated to be synergistic with currently used antiviral agents in vitro, this work compels further investigations into the potential benefits of incorporation of CCZ derivatives into contemporary antiviral regimens in humans, moving towards improving the efficacy, affordability, and accessibility of treatment.

Supplementary Data

Supplementary materials are available at *The Journal of Infectious Diseases* online. Consisting of data provided by the authors to benefit the reader, the posted materials are not copyedited and are the sole responsibility of the authors, so questions or comments should be addressed to the corresponding author.

Notes

Acknowledgments. We thank P. Shinn, M. Itkin, and Z. Itkin for help with compound management.

Financial support. This work was supported by the Intramural Research Programs of the National Institute of Diabetes and Digestive and Kidney Diseases and the National Center for Advancing Translational Sciences.

Potential conflicts of interest. S. H., Z. H., J. J. M., and T. J. L. are named as inventors on a patent related to antihistamines and heterocyclic compounds for the treatment of HCV. The other authors declare that they have no potential conflicts of interest. All authors have submitted the ICMJE Form for Disclosure of Potential Conflicts of Interest. Conflicts that the editors consider relevant to the content of the manuscript have been disclosed.

References

1. Mohd Hanafiah K, Groeger J, Flaxman AD, Wiersma ST. Global epidemiology of hepatitis C virus infection: new estimates of age-specific antibody to HCV seroprevalence. Hepatology **2013**; 57:1333–42.
2. Poordad F, McCone J Jr, Bacon BR, et al.; SPRINT-2 Investigators. Boceprevir for untreated chronic HCV genotype 1 infection. N Engl J Med **2011**; 364:1195–206.
3. Liang TJ, Ghany MG. Current and future therapies for hepatitis C virus infection. N Engl J Med **2013**; 368:1907–17.
4. Afdhal N, Zeuzem S, Kwo P, et al.; ION-1 Investigators. Ledipasvir and sofosbuvir for untreated HCV genotype 1 infection. N Engl J Med **2014**; 370:1889–98.
5. Lawitz E, Mangia A, Wyles D, et al. Sofosbuvir for previously untreated chronic hepatitis C infection. N Engl J Med **2013**; 368:1878–87.
6. Backus LI, Belperio PS, Shahoumian TA, Loomis TP, Mole LA. Real-world effectiveness of ledipasvir/sofosbuvir in 4365 treatment-naive, genotype 1 hepatitis C-infected patients. Hepatology **2016**; 64:405–14.
7. Terrault NA, Zeuzem S, Di Bisceglie AM, et al. Effectiveness of ledipasvir-sofosbuvir combination in patients with hepatitis C virus infection and factors associated with sustained virologic response. Gastroenterology **2016**; 151:1131–40.e5.
8. Belperio PS, Hwang EW, Thomas IC, Mole LA, Cheung RC, Backus LI. Early virologic responses and hematologic safety of direct-acting antiviral therapies in veterans with chronic hepatitis C. Clin Gastroenterol Hepatol **2013**; 11:1021–7.
9. Yee BE, Nguyen NH, Jin M, Lutchman G, Lim JK, Nguyen MH. Lower response to simeprevir and sofosbuvir in HCV genotype 1 in routine practice compared with clinical trials. BMJ Open Gastroenterol **2016**; 3:e000056.
10. Backus LI, Belperio PS, Shahoumian TA, Loomis TP, Mole LA. Effectiveness of sofosbuvir-based regimens in genotype 1 and 2 hepatitis C virus infection in 4026 U.S. Veterans. Aliment Pharmacol Ther **2015**; 42:559–73.
11. Maan R, van Tilborg M, Deterding K, et al. Safety and effectiveness of direct-acting antiviral agents for treatment of patients with chronic hepatitis C virus infection and cirrhosis. Clin Gastroenterol Hepatol **2016**; 14:1821–30.e6.
12. Vernaz N, Girardin F, Goossens N, et al. Drug pricing evolution in hepatitis C. PLoS One **2016**; 11:e0157098.
13. Ferenci P, Bernstein D, Lalezari J, et al.; PEARL-III Study; PEARL-IV Study. ABT-450/r-ombitasvir and dasabuvir with or without ribavirin for HCV. N Engl J Med **2014**; 370:1983–92.
14. He S, Lin B, Chu V, et al. Repurposing of the antihistamine chlorcyclizine and related compounds for treatment of hepatitis C virus infection. Sci Transl Med **2015**; 7:282ra49.
15. He S, Xiao J, Dulcey AE, et al. Discovery, optimization, and characterization of novel chlorcyclizine derivatives for the treatment of hepatitis C virus infection. J Med Chem **2016**; 59:841–53.
16. Gottwein JM, Jensen TB, Mathiesen CK, et al. Development and application of hepatitis C reporter viruses with genotype 1 to 7 core-nonstructural protein 2 (NS2) expressing fluorescent proteins or luciferase in modified JFH1 NS5A. J Virol **2011**; 85:8913–28.

17. Shah P, Kerns E, Nguyen DT, et al. An automated high-throughput metabolic stability assay using an integrated high-resolution accurate mass method and automated data analysis software. Drug Metab Dispos **2016**; 44:1653–61.
18. Sun H, Nguyen K, Kerns E, et al. Highly predictive and interpretable models for PAMPA permeability. Bioorg Med Chem **2017**; 25:1266–76.
19. Kan H, Hiraga N, Imamura M, et al. Combination therapies with daclatasvir and asunaprevir on NS3-D168 mutated HCV in human hepatocyte chimeric mice. Antivir Ther **2016**; 21:307–15.
20. Lok AS, Gardiner DF, Lawitz E, et al. Preliminary study of two antiviral agents for hepatitis C genotype 1. N Engl J Med **2012**; 366:216–24.
21. Hu Z, Lan KH, He S, et al. Novel cell-based hepatitis C virus infection assay for quantitative high-throughput screening of anti-hepatitis C virus compounds. Antimicrob Agents Chemother **2014**; 58:995–1004.
22. Hu Z, Hu X, He S, et al. Identification of novel anti-hepatitis C virus agents by a quantitative high throughput screen in a cell-based infection assay. Antiviral Res **2015**; 124:20–9.
23. Steinmann E, Pietschmann T. Cell culture systems for hepatitis C virus. Curr Top Microbiol Immunol **2013**; 369:17–48.
24. Lin B, He S, Yim HJ, Liang TJ, Hu Z. Evaluation of antiviral drug synergy in an infectious HCV system. Antivir Ther **2016**; 21:595–603.
25. Pietschmann T. Clinically approved ion channel inhibitors close gates for hepatitis C virus and open doors for drug repurposing in infectious viral diseases. J Virol **2017**; 91:e01914–16.
26. Kazmi F, Hensley T, Pope C, et al. Lysosomal sequestration (trapping) of lipophilic amine (cationic amphiphilic) drugs in immortalized human hepatocytes (Fa2N-4 cells). Drug Metab Dispos **2013**; 41:897–905.
27. Goldman SD, Funk RS, Rajewski RA, Krise JP. Mechanisms of amine accumulation in, and egress from, lysosomes. Bioanalysis **2009**; 1:1445–59.